

# Modular and Portable Time-Resolved Fluorescence Measurement System

Raphael Hagen\*, Fabrizio Spano\*, Mathias Bonmarin\* and Daniel Fehr\*

\*Institute of Computational Physics, ZHAW Zurich University of Applied Sciences, Winterthur, Switzerland  
 {raphael.hagen, fabrizio.spano, mathias.bonmarin, daniel.fehr}@zhaw.ch,

**Abstract**—Time-resolved fluorescence measurements are not only able to overcome the limitations of intensity-based applications, but can also resolve information about the sample that is not possible with steady-state data. As monitoring-based preventive medicine becomes more popular, efforts have been made to develop smaller and more affordable measurement methods that could potentially be integrated into point-of-care devices. In this work, we present a portable, low-cost demonstration device that can perform time-resolved fluorescence measurements in the frequency domain. The device combines the flexibility and advanced measurement modes of a desktop sensor system with the small form factor of a portable point-of-care device. Initial measurements show promising results, but further testing is needed to fully assess the performance of the device.

**Index Terms**—Time-resolved fluorescence, frequency-domain, portable, silicon photomultiplier, heterodyne

## I. INTRODUCTION

Advances in the development of fluorometric assays during the last century have paved the way for the now widespread use of fluorescence measurement techniques [1]. Modern measurement systems are extremely sensitive and provide information on changes in the optical properties of analytes, including fluorescence intensity, wavelength shift, polarization (anisotropy decay), or lifetime. As a result, they are finding wide acceptance in biomedical and environmental applications [2], [3]. The wide range of applications for time-resolved fluorometric assays has led to the development of various measurement systems. In the last two decades, the development of portable and low-cost time-domain (TD) and frequency-domain (FD) meters has increased, following the trend of point-of-care (POC) applications [4]–[10]. However, these measurement devices are often application-specific and do not provide the flexibility of desktop systems. In this study, we sought to develop an instrument for time-resolved fluorescence measurement that combines the advantages of both worlds. A device with the flexibility and measurement modes of a desktop system combined with the low-cost and small form factor of POC devices.

## II. MEASUREMENT SYSTEM

The developed measuring device consists of two components, the excitation module and the detection module. Both modules can be operated independently, i.e. the excitation module in combination with other detectors or the detection module in combination with other light sources. In the interlinked mode, both modules form a compact measurement system

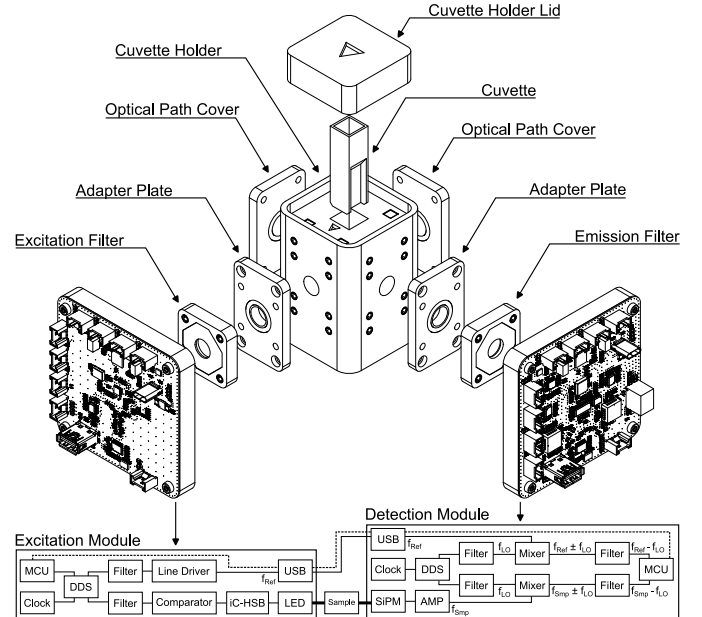


Fig. 1. Top: this example is 3D printed and can be used to characterize liquid samples in a semi-microcuvette. Bottom: block diagram of the signal paths, communication link and heterodyning signal processing concept.

that can measure time-resolved fluorescence. In all cases, the modules are controlled and powered by a computer. The system configuration is shown in Fig. 1. The main features that allow to combine the most important aspects of a desktop instrument and a POC device are explained in the following sections.

The driver for the laser diode (iC-HSB, iC-Haus, Germany) is the core component of the excitation module. The internal pulse generator of the driver is capable of generating pulses with a full width-half max (FWHM) of 100 ps up to 5 ns with a resolution of 1 ps. The repetition rate (0–25 MHz) of the pulses is controlled by the trigger signal of the local direct digital synthesis (DDS) (AD9834, Analog Devices, USA). Disabling the internal pulse generator, connects the trigger input signal to the output, allowing square wave modulation. The iC-HSB has three driver stages that provide an output current of up to 300 mA to support a larger number of light sources.

The chosen detector technology is the silicon photomultiplier (SIPM), which can be operated with simple front-end electronics and seemed to be the most future-proof concept. A SIPM detector combines a series of single photon avalanche diode (SPAD) microcells. SIPMs with small (about 10  $\mu\text{m}$ )

several hundred microcells achieve bandwidths up to 60 MHz, SIPMs with large (about 100  $\mu\text{m}$ ) several thousand microcells achieve internal gains up to  $10^6$ . The system supports SIPMs with a bias voltage of 0 – 80 V. The detector is soldered to a small adapter board connected to the detection module, allowing easy adaptation to high-speed or high-sensitivity SIPMs.

The detection module uses the heterodyning technique, which multiplies the high frequency (HF) input signals  $f_{\text{Ref}}$  and  $f_{\text{Smp}}$  with a signal  $f_{\text{LO}}$  from the local DDS, resulting in synchronized output signals with frequencies  $f_{\text{Ref}} \pm f_{\text{LO}}$  and  $f_{\text{Smp}} \pm f_{\text{LO}}$ . Low-pass filtering of the output signals suppresses the HF sum and allows only the ultra low frequency (ULF) difference to pass. The phase delay between the two down-converted signals is proportional to the apparent lifetime of the sample. The block diagram of the heterodyning concept is shown in Fig. 1.

The optical configuration can be freely designed according to the measurement task. The upper part of Fig. 1 shows a possible design example used to characterize liquid samples in a semi-microcuvette. This setup is printed entirely from polylactide (PLA) using a standard fused deposition modeling (FDM) 3D printer.

### III. EVALUATION

In this initial instrument evaluation, the developed measurement system will investigate time-resolved fluorescence measurements based on a potential of hydrogen (pH)-sensitive acridine marker. Acridine is among the indicators with the largest pH response [11]–[13]. A lifetime of about 10 ns for neutral acridine ( $\text{Ac}^-$ ) and a lifetime of 31 ns for protonated acridine ( $\text{Ac}_{\text{H}^+}$ ) are reported by [14]–[16]. Time-resolved measurements are usually made between 440 – 500 nm, the range in which both species emit and in which the apparent lifetime is directly related to pH [14, Fig. 7.49]. For measurements with an acridine-based pH indicator, an optical setup with a  $90^\circ$  orientation is chosen, which significantly reduces the transmission of excitation light to the detector. An optical bandpass filter with a central wavelength of 375/10 nm (Edmund Optics, USA) (the second number is the FWHM of the filter) is placed behind the light-emitting diode (LED) (MT5375-UV, Marktech Optoelectronics, USA). An emission filter with a central wavelength of 500/24 nm (Edmund Optics, USA) is placed in front of the SIPM (13360-3025CS, Hamamatsu, Japan) detector. The sample is excited by a pulse modulated signal with a repetition rate of 4 MHz and a FWHM of 5 ns. The 4 MHz modulation signal is down-converted to 500 Hz to digitize and calculate the pH-related phase delay using an microcontroller (MCU) (RP2040, Raspberry Pi Foundation, England UK).

#### A. Sample Preparation

The chemicals used to prepare the samples, such as acridine (No: A23609), potassium phosphate (No: P0662), and dibasic potassium phosphate (No: P8281), were purchased from Merck (Germany).

The 0.1 M aqueous phosphate buffer solutions were mixed according to the instructions described in [17, p. 152, p. 153]. First, two 1-liter base solutions of potassium phosphate mono

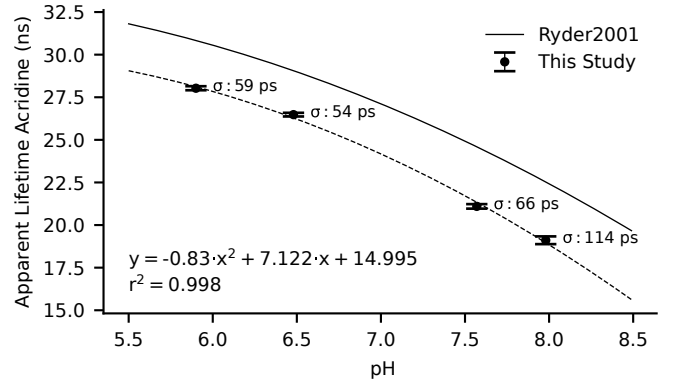


Fig. 2. Measurements of apparent lifetime with the developed device compared to [11]. Both curves show a decrease in lifetime as a function of pH. At lower pH, emission from the long-lived  $\text{Ac}_{\text{H}^+}$  species dominates; at higher pH, the ratio between  $[\text{Ac}^-]$  and  $[\text{Ac}_{\text{H}^+}]$  changes and the contribution to the emission from  $\text{Ac}^-$  increases, leading to a decrease in apparent lifetime.

and di-potassium salt solutions were prepared. For the mono-potassium base solution, 27.2 g monobasic potassium phosphate ( $\text{KH}_2\text{PO}_4$ ) was dissolved in 500 ml deionized water and adjusted to 1 liter with deionized water. For the di-potassium base solution, 34.8 g dibasic potassium phosphate ( $\text{K}_2\text{HPO}_4$ ) was dissolved in 500 ml deionized water and adjusted to 1 liter with deionized water. To obtain 200 ml of 0.1 M K-phosphate solutions with different pH values, certain volumes of the two base solutions were mixed together. Four solutions in the pH range 5 – 8 were prepared. Acridine was added to each solution at a concentration of 0.001 M. Then, the exact pH value of each solution was measured using a Mettler Toledo FiveEasy F20 with an LE438 probe. Finally, 1 ml of each solution is transferred to a separate semi-microcuvette to form a sample.

#### B. Results

The apparent lifetime measured with the developed device shows a decrease as a function of pH, see Fig. 2. At a pH of 6, the emission is dominated by  $\text{Ac}_{\text{H}^+}$ , resulting in an apparent lifetime of almost 31 ns. As the pH value increases, the ratio between  $[\text{Ac}^-]$  and  $[\text{Ac}_{\text{H}^+}]$  changes, decreasing the apparent lifetime of the sample. In the measured range of pH 6-8, the change in lifetime corresponds to a 2<sup>nd</sup> polynomial and allows the calculation of pH based on the measured apparent lifetime. Based on the measured standard deviation of each point, one could predict an accuracy of  $\text{pH} \pm 0.032$  (95 % probability interval of  $\pm 2\sigma$ ).

A comparison of the measurements made in this study with [11] yields a parallel curve with an offset, see Fig. 2. This offset in the apparent lifetime is due to the early development stage of our device, where some characterization parameters related to heterodyning performance and delays caused by electronics in general are still missing. Nevertheless, the measurements show promising signs that the device concept works and is able to adapt to a specific measurement task and measure time-resolved fluorescence.

#### IV. CONCLUSION

The device developed in this work attempts to combine the advantages of desktop systems for time-resolved fluorescence measurements with the cost and size advantages of POC devices. The device is capable of many modulation modes and supports a variety of SIPM detectors. In the heterodyne detection used, the HF modulation of the sample is down-converted to a ULF signal, which is directly digitized by the on-chip digital to analog converter (ADC) of the MCU.

Further testing is needed to fully evaluate the device's performance. It could provide researchers with an affordable, portable, and versatile system for time-resolved fluorescence measurements.

#### ACKNOWLEDGMENTS

R.H., F.S., M.B. and D.F. gratefully acknowledge financial support from the ZHAW School of Engineering.

#### REFERENCES

- [1] I. Hemmilä and S. Webb, "Time-resolved fluorometry: an overview of the labels and core technologies for drug screening applications," *Drug Discovery Today*, vol. 2, pp. 373–381, Sept. 1997.
- [2] W. Becker, "Fluorescence lifetime imaging – techniques and applications," *Journal of Microscopy*, vol. 247, no. 2, pp. 119–136, 2012.
- [3] D. P. Millar, "Time-resolved fluorescence spectroscopy," *Current Opinion in Structural Biology*, vol. 6, pp. 637–642, Oct. 1996.
- [4] J. Kissinger and D. Wilson, "Portable Fluorescence Lifetime Detection for Chlorophyll Analysis in Marine Environments," *IEEE Sensors Journal*, vol. 11, pp. 288–295, Feb. 2011.
- [5] J. Guo and S. Sonkusale, "A single chip fluorometer for fluorescence lifetime spectroscopy in 65nm CMOS," in *2011 IEEE SENSORS*, pp. 766–769, Oct. 2011. ISSN: 1930-0395.
- [6] C. C. Sthalekar and V. J. Koomson, "A CMOS Sensor for Measurement of Cerebral Optical Coefficients Using Non-Invasive Frequency Domain Near Infrared Spectroscopy," *IEEE Sensors Journal*, vol. 13, pp. 3166–3174, Sept. 2013.
- [7] J. Lagarto, J. D. Hares, C. Dunsby, and P. M. W. French, "Development of Low-Cost Instrumentation for Single Point Autofluorescence Lifetime Measurements," *Journal of Fluorescence*, vol. 27, pp. 1643–1654, Sept. 2017.
- [8] H. Wang, Y. Qi, T. J. Mountziaris, and C. D. Salthouse, "A portable time-domain LED fluorimeter for nanosecond fluorescence lifetime measurements," *Review of Scientific Instruments*, vol. 85, p. 055003, May 2014.
- [9] O. Alonso, N. Franch, J. Canals, K. Arias-Alpizar, E. de la Serna, E. Baldrich, and A. Diéguez, "An internet of things-based intensity and time-resolved fluorescence reader for point-of-care testing," *Biosensors and Bioelectronics*, vol. 154, p. 112074, Apr. 2020.
- [10] D. Xiao, Z. Zang, N. Sapermsap, Q. Wang, W. Xie, Y. Chen, and D. D. U. Li, "Dynamic fluorescence lifetime sensing with CMOS single-photon avalanche diode arrays and deep learning processors," *Biomedical Optics Express*, vol. 12, pp. 3450–3462, June 2021.
- [11] A. Ryder, S. Power, T. Glynn, and J. Morrison, "Time-domain measurement of fluorescence lifetime variation with pH," vol. 4259, pp. 102–109, July 2001.
- [12] A. Ryder, S. Power, and T. Glynn, "Evaluation of Acridine in Nafion as a Fluorescence-Lifetime-Based pH Sensor," *Applied spectroscopy*, vol. 57, pp. 73–9, Feb. 2003.
- [13] C. Totland, P. Thomas, B. Holst, N. Akhtar, J. Hovdenes, and T. Skodvin, "The use of surfactant-filled mesoporous silica as an immobilising medium for a fluorescence lifetime pH indicator, providing long-term calibration stability," *RSC Advances*, vol. 9, pp. 37241–37244, Nov. 2019.
- [14] J. R. Lakowicz, *Principles of Fluorescence Spectroscopy*. Boston, MA: Springer US, 2006.
- [15] A. Gafni and L. Brand, "Excited state proton transfer reactions of acridine studied by nanosecond fluorometry," *Chemical Physics Letters*, vol. 58, pp. 346–350, Oct. 1978.
- [16] J. R. Lakowicz and A. Balter, "Analysis of excited-state processes by phase-modulation fluorescence spectroscopy," *Biophysical chemistry*, vol. 16, pp. 117–132, Oct. 1982.
- [17] R. A. Science, *Lab FAQs, Find a Quick Solution*. Roche Diagnostics GmbH, Roche Applied Science, 68298 Mannheim, Germany, 3 ed., 2017.